Performing Joint Measurements on Electron Spin Qubits by Measuring Current through a Nearby Conductance Channel

Kevin S. Huang

Centennial High School, Ellicott City, MD

Abstract

Advances in the manufacturing of semiconductor structures have allowed the observation of electron spins which are potentially useful for the construction of quantum computers. This project probes a new direction by theoretically exploring the procedure to perform joint measurements on spatially separated spin qubits through measuring the current in a nearby conductance channel. These joint measurements can be used to facilitate entanglement and form the basis of fault-tolerant error correction procedures. The main concept is to use a singlet-triplet qubit formed by a double quantum dot with tunable bias such that the charge density shifts in a spin-dependent way. As a result, electrostatic coupling between the qubits and conductance channel creates a scattering potential that depends on the spin states of the trapped electrons. Theoretical conditions must be taken into account before this can actually be implemented in experiment. In modeling this procedure through a transfer matrix approach, it is demonstrated that such measurements can be performed in principle although there are experimental limitations due to increasing sensitivity in barrier parameters and noise. The results and conclusions of this project lay the foundation for further paths of exploration in realistic models to calculate the constraints of performing this joint measurement.

Keywords: quantum computer, joint measurement, entanglement, singlet-triplet qubit, scattering

Performing Joint Measurements on Electron Spin Qubits by Measuring Current through a Nearby Conductance Channel

I. Introduction

Quantum computation holds significant potential as a computing paradigm beyond classical silicon-based computing. It offers immense advantages in efficiently solving problems such as integer factorization, combinatorial optimization, and quantum simulation that are infeasible for classical computers. However, quantum computation is difficult due to its “closed box” requirement. While the programmer can control a quantum computer's internal operation, it must otherwise be isolated from the rest of the universe (Ladd et al. 2010). Small amounts of interference can disturb the fragile quantum wavefunctions, causing the destructive process known as decoherence. DiVincenzo performed a seminal work to characterize the physical requirements for an implementation of a fault-tolerant quantum computer (DiVincenzo 2000). His original considerations can be classified under three general criteria: scalability, universal logic and correctability. The major barrier to building quantum computers is maintaining the simultaneous abilities to control quantum systems, measure them, and preserve their strong isolation from uncontrolled parts of their environment. Because noise and decoherence have been substantial obstacles to realizing quantum computers that are reliably controlled and scalable, this project aimed to develop a new, efficient procedure to perform joint measurements on electron spin qubits. A joint measurement on multiple qubits gives information on the state of the system without revealing the individual state of each qubit. These joint measurements have applications in two key areas: facilitating entanglement and forming the basis of error-correction procedures.

The means of entangling the spins is currently limited to either superexchange via direct tunnel coupling, which is short ranged and requires dense, tunable, technically challenging gate arrays, or Coulomb interaction, which is weak and susceptible to noise at long distance. The ability to use joint measurements to entangle qubits is a well-known idea in the linear optical computing due to the Knill-Laflamme-Milburn proposal that demonstrated efficient quantum computation is possible using photons, linear optical elements, and projective measurements (Knill et al. 2001; Kok et al. 2007). The

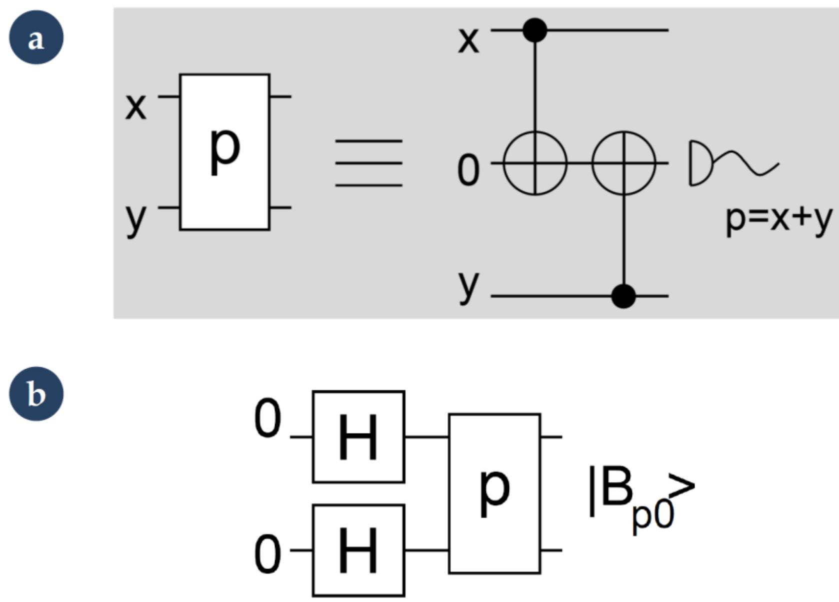

Figure 1. (a) Quantum circuit representation of a parity gate and (b) straightforward entanglement of two qubits in pure states (Image from Ionicioiu, 2007).

KLM scheme has progressed from a mathematical proof-of-concept to practical realization, through simple quantum algorithms and theoretical developments (O'Brien 2007; Politi et al. 2009). The basis of quantum error correction is the parity measurement which can be found in the bit flip, phase flip, and Shor code. The four-qubit joint measurement is especially relevant for Steane's 7-qubit code (Steane 1996) and the perfect five-qubit code (DiVincenzo and Shor 1996; Laflamme et al. 1996; Nielsen and Chuang 2011). These joint measurements are typically envisioned to be carried out with a series of two-qubit operations between data qubits and ancillas, but the direct approach used in this procedure would simplify the process to a single measurement.

Both resonant tunneling and measurement-based quantum information processing are well-established ideas that have been studied previously. However, they have not been placed in the context of each other in published literature. This combination of simple ideas immediately raises interesting and fundamental theoretical questions and lends itself to the novelty of this work. In this project, a scheme is first presented that would allow joint measurements, specifically parity gates (Figure 1), to be implemented in solid state electronics. Such a parity gate projects a general two qubit state to a subspace of even or odd parity (Beenakker et al. 2004; Ionicioiu 2007). The objective of this project is to consider this idea to implement joint measurements on electron spins and evaluate its experimental feasibility. It began from finding the theoretical requirements for conductance measurements to distinguish between different parity states of a multi-qubit system without resolving the individual states. This project included modeling the potential barrier heights, inter-qubit distances, the width of resonance, incident energy, and the energy spread of transport electrons. It is important to note that a theoretical model must be developed and tested before this procedure can be implemented in experiment. In modeling this procedure through a transfer matrix approach (Ando and Itoh 1987; Deinega et al. 2013), the project demonstrated that such joint measurements were able to be performed in principle, although there were experimental limitations due to increasing sensitivity in barrier parameters and noise.

II. Theoretical Model

The backbone of this scheme is utilizing quantum tunneling phenomena to distinguish between different states of a multi-qubit system. In analyzing a time-independent model of transport, electrons in the channel are a superposition of plane waves moving right and left in satisfying Schrodinger's equation (Figure 2).

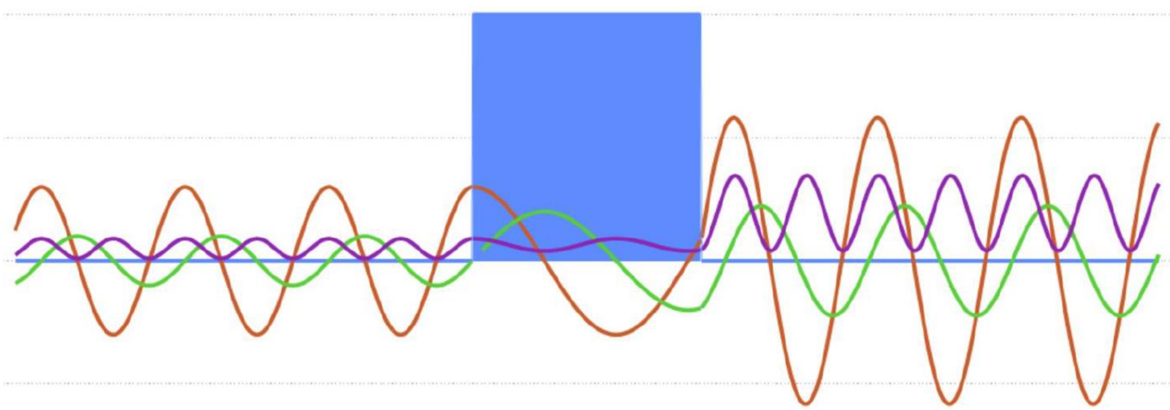

Figure 2. Scattering across a rectangular barrier. The real part is orange, the imaginary part is green, and the square of the wavefunction is purple (Image from Competition Entrant).

$$-\frac{\hbar^2}{2m}\frac{d^2\psi}{dx^2} + V\psi(x) = E\psi(x)$$

$$\psi(x) = Ae^{ikx} + Be^{-ikx}$$

$$k = \sqrt{\frac{2m(E-V)}{\hbar^2}}$$

By enforcing the continuity conditions at the boundaries between barriers, one can calculate the transmission of particles across potential barriers. Because the outgoing amplitudes can be obtained in terms of incoming amplitudes, the transmission across multiple potential barriers can thus be generalized to an effective transfer matrix

(Ando and Itoh 1987; Deinega et al. 2013). This allows for the numerical calculation of transmission across potential barriers of arbitrary shape.

$$\begin{pmatrix} C_{n1} \\ C_{n2} \end{pmatrix} = M_{n-1} M_{n-2} \ldots M_2 M_1 M_0 \begin{pmatrix} C_{11} \\ C_{12} \end{pmatrix}$$

$$M_m = \begin{pmatrix} \frac{k_{m+1} + k_m}{2k_{m+1}} e^{-i(k_{m+1} - k_m)d} & \frac{k_{m+1} - k_m}{2k_{m+1}} e^{-i(k_{m+1} + k_m)d} \\ \frac{k_{m+1} - k_m}{2k_{m+1}} e^{i(k_{m+1} + k_m)d} & \frac{k_{m+1} + k_m}{2k_{m+1}} e^{i(k_{m+1} - k_m)d} \end{pmatrix}$$

$$T = \frac{|F|^2}{|A|^2} = \frac{|M|^2}{|M_{22}|^2}$$

$$R = \frac{|B|^2}{|A|^2} = \frac{|M_{21}|^2}{|M_{22}|^2}$$

Gallium arsenide (GaAs) is a compound of the elements gallium and arsenic. It is a III-V direct bandgap semiconductor with a zinc blende crystal structure. The effective mass of an electron in GaAs as well as the effective permittivity were taken into account in modeling scattering. A quantum point contact (QPC) is a narrow constriction between two electrically conducting regions, of width comparable to the electron wavelength. QPC were independently reported in 1988 by two groups (van Wees et al. 1988; Wharam et al. 1988), based on their earlier work in silicon and then in GaAs (Dean and Pepper 1982; Berggren et al. 1986; Thornton et al. 1986). A quantum dot (Figure 3) is an artificial GaAs heterostructure that holds an electron whose spin projection can be used as a physical qubit. Consider two unequal reservoirs in separate regions of a two-dimensional electron gas (2DEG) held at different Fermi levels by voltage leads to permit charge transport (Figure 3 a, c and d). An effective one-dimensional conductance channel, which connects the two reservoirs, is assumed to be disorder-free. A singlet-triplet qubit is formed by two electrons in a double quantum dot with tunable bias. This coupling involves a temporary spin-to-charge conversion via Pauli spin blockading similar to readout techniques of singlet-triplet qubits (Figure 3b) already coupled to a quantum point contact (Hanson et al. 2007). For a 1D channel in a GaAs heterostructure, the ideal electric potential induced by a coupled qubit is:

$$V_1(x) = \frac{\delta e}{e}\frac{e^2}{4\pi\varepsilon}\left(\frac{1}{\sqrt{x^2+l'^2}} - \frac{1}{\sqrt{x^2+l^2}}\right)$$

where it is assumed the spins are placed in dots L=200 nm away from the channel and

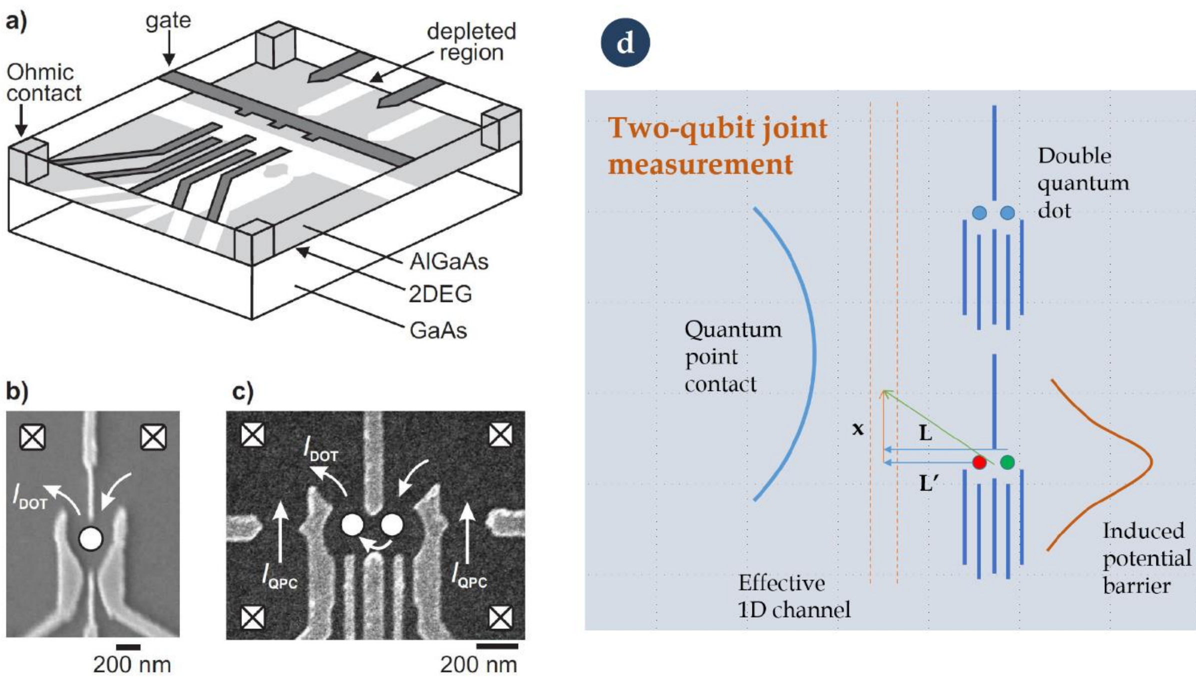

Figure 3. Quantum dot. (a) Voltages applied by gate electrodes (dark gray) deplete regions in a two-dimensional electron gas (2DEG). (b) White dots indicate location of the electrons. (c) Current passing through the quantum point contact will be measured (Images a, b, and c from Hanson et al., 2007). (d) Schematic diagram for two-qubit joint measurement (Image d from Competition Entrant).

turning up the inter-dot bias voltage results in a fraction δe/e of the charge density tunneling into a dot L’ = 100 nm away. The result is that upon adjusting a gate voltage, the charge density will shift in a spin-dependent way so that information will be temporarily stored in the charge configuration. Thus, electrostatic coupling between the qubits and conductance channel creates a scattering potential for transport electrons that depends on the spin states of the trapped electrons.

III. Materials and Methods

<u>Resonant Tunneling</u>

Transmission resonances depend on the joint state of all trapped spins. In the case of two qubits, there is a resonant height of the double-barrier potential which yields perfect transmission (Figure 4). Differences in transmission allow for an experimental measurement of current passing through the channel to distinguish between the two states. A measurement of conductance will give only 0 or 1, although there are four possible spin states. This joint measurement indicates whether both spins are in the same direction, but does not distinguish between whether they are both up or both down i.e. it does not collapse the wavefunction within a given parity subspace. It is interesting to note that the two-qubit check can be directly extended to the N-qubit case

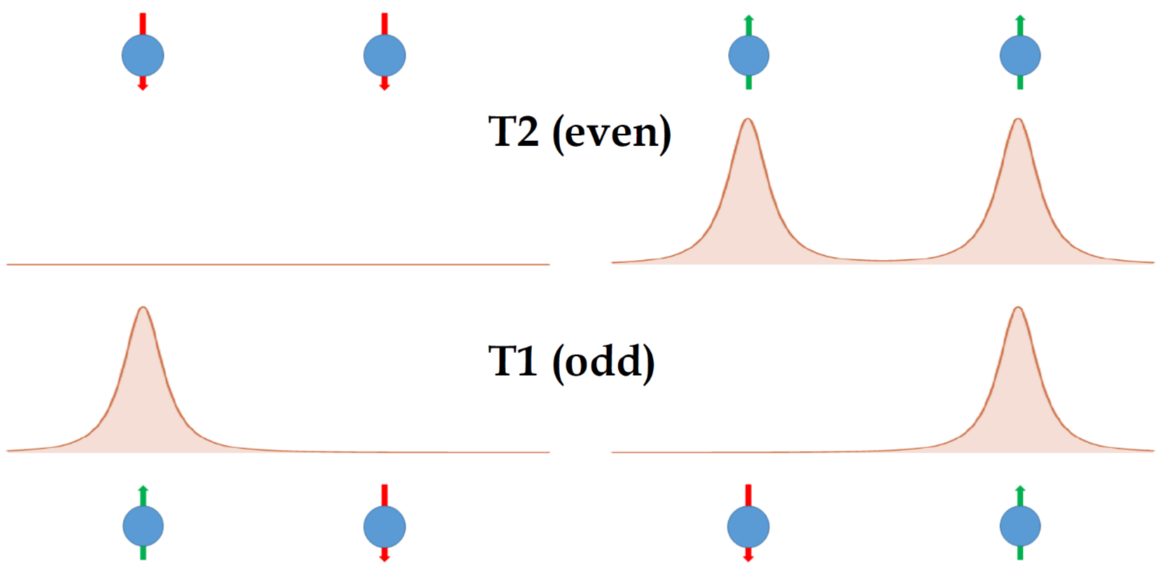

Figure 4. Resonant tunneling across two barriers will result in the same transmission for even parity states. Transmission across one barrier should be distinguishably smaller. Electron spins are shown for illustrative purposes only (Image from Competition Entrant).

(Rozman et al. 1994). In this study, transmission was calculated in approximating the Coulomb barrier with n = 100 rectangular barriers. Numerical calculations were carried out using MATLAB while some figures were generated in Mathematica.

Realistic Constraints

The experimental constraints on distance sensitivity limit precision to 5-10 nm. Similarly, the spread in the electrons' energy is constrained by the lowest temperatures achievable in dilution refrigerators with typical base temperatures around 20 mK (Hanson et al. 2007). For purposes of distinguishability, the state-of-the-art devices can detect deviations in current through the quantum point contact down to 1% (absolute deviation of 0.3 nA) which will be set as the critical value (Vandersypen et al. 2004; Reilly et al. 2007).

Quantum Transport

A nanostructure taking part in quantum transport is within an electric circuit. At equilibrium, the average number of electrons in any energy level is described by the Fermi function. Applying a voltage across the source and the drain maintains two distinct electrochemical potentials which gives rise to two different Fermi functions (Nazarov and Blanter 2009). Current flows through the channel due to this energy difference in an attempt to restore equilibrium. In using a scattering theory of transport, the Landauer formula can be used to calculate conductance *G* across a small-bias channel (where the infinitesimal difference in Fermi level gives rise to the thermal broadening function F_T) (Datta 2005).

$$G = \left(\frac{q^2}{h}\right) T_0$$

$$T_0 \equiv \int_{-\infty}^{+\infty} dE\ \bar{T}(E)\ F_T(E-\mu)$$

Conceptually, current is calculated from the energy distribution of transport electrons amplified by the transmission distribution $\bar{T}(E)$, which represents the proportion of electrons that pass through at a given energy. This will be utilized as the link between the transmission across potential barriers to the measurement of current through the QPC in an experiment.

Competition Entrant's Personal Role in This Work

Mentor helped to choose this project based upon Competition Entrant's interest as well as referred Competition Entrant to the relevant literature in gaining the necessary background information. Under Mentor's guidance for research direction, Competition Entrant designed the scheme and developed the theoretical modeling for the multi-barrier scattering potential. Competition Entrant set up the calculations to search for solutions subject to the constraints. Competition Entrant analyzed results, plotted figures, prepared poster, and wrote the research report.

IV. Results and Discussion

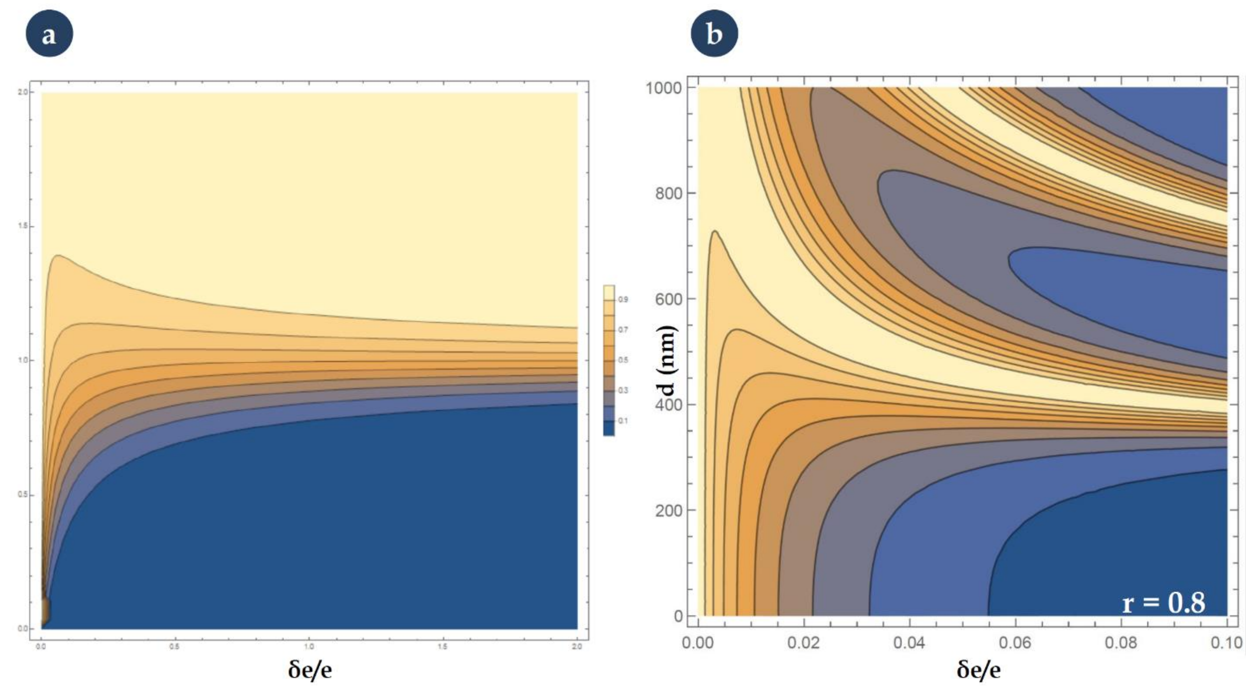

Figure 5. (a) Transmission contour of a single barrier as a function of relative energy r = E/V and δe/e which represents absolute barrier height. (b) Transmission contour of a double barrier as a function of barrier separation and δe/e for r = 0.8 (Image from Competition Entrant).

In calculating transmission across a single barrier, Figure 5a shows how the transmission amplitude *T* (represented by intensifying colors on this contour plot) changes with *δe/e*, the fraction of charge which shifts and determines the barrier height, and *r*, the relative incident energy of transport electrons. It is noted that while energy increases with transmission, larger *δe/e* corresponds to a faster increase. Because barrier distance *d* can be adjusted to allow for near resonant transmission in the even parity case (Figure 5b), it is important to identify the region in which *T*(*δe/e, r*) < 1 for the single barrier (or in general, odd parity) case.

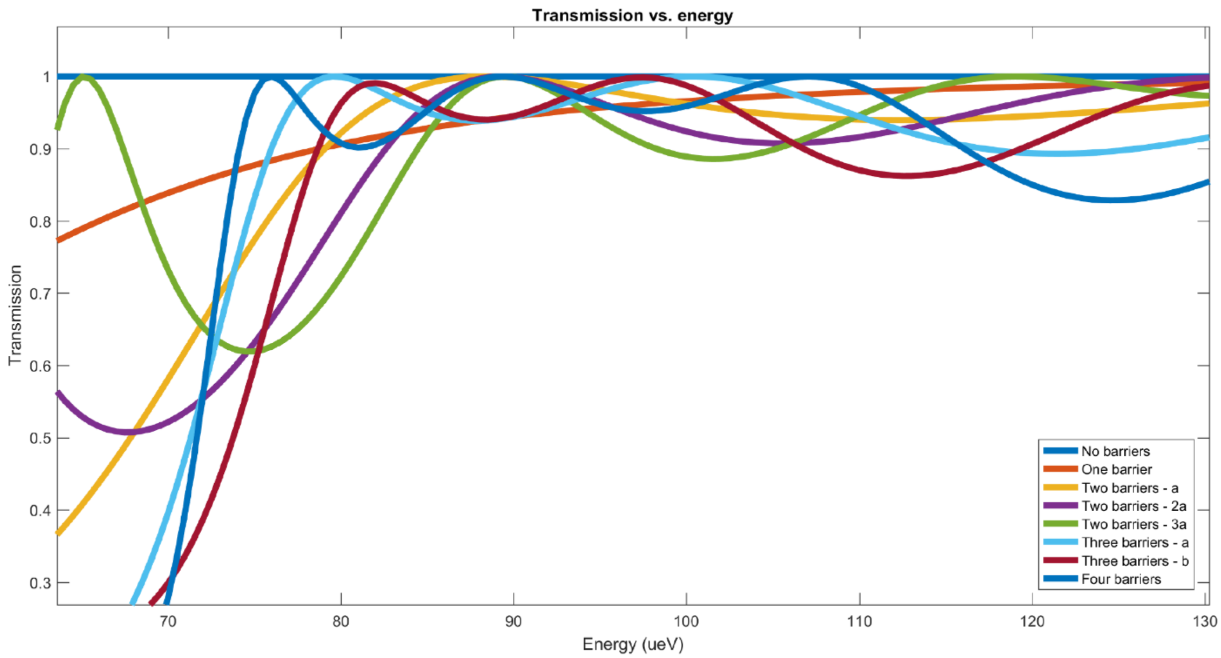

Figure 6. Transmission as a function of energy for all barrier combinations for four qubits. The two barriers “a” plot represents the transmission across two barriers separated by the smallest resonant distance, 1a. Similarly, the “2a” and “3a” plots represent separations of 2a and 3a. The three barriers “a” plot represents the transmission across three barriers separated by 1a. The three barriers “b” plot represents the transmission across two barriers separated by 1a and the third barrier a distance 2a away. The four barriers plot represents the transmission across all four barriers. (Image from Competition Entrant).

In an attempt to maximize tolerance in distance and energy, a compromise between distance and energy sensitivity is observed. As the barrier height is increased, the sensitivity in distance increases and the sensitivity to energy decreases (Figure 5). When the transmission difference between even and odd parity states is increased by lowering the energy of incident electrons, the resonance peak narrows and stricter stability is required in the parameter values to observe the interference effect. In this preliminary modeling, transport electrons need to have energies controlled with high precision to avoid distinguishing between states of the same parity.

Table 1. Sample result for four-qubit joint measurement as shown in Figure 6.

Set-up conditions: T = 10 mK, d = 500 nm, δe/e = 0.08, E = 88 ueV
Relative conductances ($\frac{G}{e^2/h}$)
Even parity: G0 = 1.000, G2a = 0.998, G2b = 0.991, G2c = 0.981, G4 = 0.989
Odd parity: G1 = 0.938, G3a = 0.942, G3b = 0.945

Figure 6 shows the transmission amplitude as a function of incident energy for a sample four-qubit joint measurement. The results for this measurement are also shown in Table 1. The five combinations in the even parity subspace consist of no barriers, two barriers (arranged at three different distances), and four barriers. The odd parity subspace consists only of one barrier and three barriers (arranged in two different combinations). The even parity relative conductances are within 1% (G0: 1.000 – G4: 0.989) and the odd parity relative conductances are within 1% (G3b: 0.945 - G1: 0.938). At the same time, the even and odd relative conductances are 4% (G4: 0.989 – G3b: 0.945) away from each other. In this case, our devices would be able to distinguish between an even and odd number of barriers to perform the projective measurement. More importantly, this measurement would not collapse the wavefunction because the conductances for all individual cases within either even or odd cases are very close together. However, the electron temperatures required are below 50 mK, beyond what can currently be achieved. Unlike rectangular barriers, the resonant distances display a general linear pattern of a+nb to the first order which leads to a discrete set of solutions, where a is a multiple of b, to achieve successful resonant tunneling in the case of more than two qubits. As expected, this procedure is also limited by the precision in which environmental parameters can be controlled. It is noted that while these joint measurements can be performed theoretically in principle, they are not yet currently accessible by experiment.

V. Conclusion and Future Direction

This project describes an initial effort in physical realization of conducting joint measurements on electron spins in quantum dot systems through resonant tunneling. The preliminary results presented here provide a basis for developing this novel scheme. For both the two-qubit and general multi-qubit joint measurement, the main challenge is dealing with the relatively large spread in the electrons' energy and small charge-coupling of qubits to the conductance channel. There is an expected increase in the sensitivity of barrier parameters as number of qubits considered increases. As a result, realistic constraints will dictate the limitations of applying this procedure to an arbitrary number of spins. The conclusions drawn here lay the foundation for further paths of exploration in realistic models to calculate constraints of performing this joint measurement. In the larger context, developing efficient quantum entanglement and error correction procedures is only one essential step to building quantum computers. Beyond this step, one must confront constraints for the relative speed of qubit-to-qubit communication, control, initialization and measurement.

Further research is needed to model the procedure in a realistic environment with detailed device modeling. The next phase in this analysis would involve modeling the 3D potential through solving Poisson's equation in a gated semiconductor geometry. This can be refined with a self-consistent Poisson-Schrodinger solver to obtain potential as a function of gate voltages and spin states. This will account for effects of gate geometry through device modeling with COMSOL. Transport across multiple channels may also need to be included. The sensitivity of the joint measurement should be calculated in the presence of imprecise gate voltages, background noise, dephasing of electrons, and decoherence during measurement to allow for an eventual experimental implementation. In realizing multi-qubit joint measurements, it would be interesting to consider their general applications to quantum information processing such as using them to create highly entangled multi-qubit states.

VI. References

Ando Y, Itoh T. 1987. Calculation of transmission tunneling current across arbitrary potential barriers. *Journal of Applied Physics* **61**: 1497-1502.

Beenakker CWJ, DiVincenzo DP, Emary C, Kindermann M. 2004. Charge Detection Enables Free-Electron Quantum Computation. *Physical Review Letters* **93**: 020501.

Berggren KF, Thornton TJ, Newson DJ, Pepper M. 1986. Magnetic Depopulation of 1D Subbands in a Narrow 2D Electron Gas in a GaAs:AlGaAs Heterojunction. *Physical Review Letters* **57**: 1769-1772.

Datta S. 2005. *Quantum transport: Atom to transistor*. Cambridge University Press, New York, NY.

Dean CC, Pepper M. 1982. The transition from two- to one-dimensional electronic transport in narrow silicon accumulation layers. *Journal of Physics C: Solid State Physics* **15**: L1287.

Deinega A, Belousov S, Valuev I. 2013. Transfer-matrix approach for finite-difference time-domain simulation of periodic structures. *Physical Review E* **88**: 053305.

DiVincenzo DP. 2000. The Physical Implementation of Quantum Computation. *Fortschritte der Physik* **48**: 771-783.

DiVincenzo DP, Shor PW. 1996. Fault-Tolerant Error Correction with Efficient Quantum Codes. *Physical Review Letters* **77**: 3260-3263.

Hanson R, Kouwenhoven LP, Petta JR, Tarucha S, Vandersypen LMK. 2007. Spins in few-electron quantum dots. *Reviews of Modern Physics* **79**: 1217-1265.

Ionicioiu R. 2007. Entangling spins by measuring charge: A parity-gate toolbox. *Physical Review A* **75**: 032339.

Knill E, Laflamme R, Milburn GJ. 2001. A scheme for efficient quantum computation with linear optics. *Nature* **409**: 46-52.

Kok P, Munro WJ, Nemoto K, Ralph TC, Dowling JP, Milburn GJ. 2007. Linear optical quantum computing with photonic qubits. *Reviews of Modern Physics* **79**: 135-174.

Ladd TD, Jelezko F, Laflamme R, Nakamura Y, Monroe C, O/'Brien JL. 2010. Quantum computers. *Nature* **464**: 45-53.

Laflamme R, Miquel C, Paz JP, Zurek WH. 1996. Perfect Quantum Error Correcting Code. *Physical Review Letters* **77**: 198-201.

Nazarov YV, Blanter YM. 2009. *Quantum transport: Introduction to nanoscience*. Cambridge University Press, New York, NY.

Nielsen MA, Chuang IL. 2011. *Quantum Computation and Quantum Information (10th Anniversary Edition)*. Cambridge University Press, New York, NY.

O'Brien JL. 2007. Optical Quantum Computing. *Science* **318**: 1567-1570.

Politi A, Matthews JCF, O'Brien JL. 2009. Shor's Quantum Factoring Algorithm on a Photonic Chip. *Science* **325**: 1221-1221.

Reilly DJ, Marcus CM, Hanson MP, Gossard AC. 2007. Fast single-charge sensing with a rf quantum point contact. *Applied Physics Letters* **91**: 162101.

Rozman MG, Reineker P, Tehver R. 1994. One-dimensional scattering: Recurrence relations and differential equations for transmission and reflection amplitudes. *Phys Rev A* **49**: 3310-3321.

Steane A. 1996. Multiple-Particle Interference and Quantum Error Correction. *Proceedings: Mathematical, Physical and Engineering Sciences* **452**: 2551-2577.

Thornton TJ, Pepper M, Ahmed H, Andrews D, Davies GJ. 1986. One-Dimensional Conduction in the 2D Electron Gas of a GaAs-AlGaAs Heterojunction. *Physical Review Letters* **56**: 1198-1201.

van Wees BJ, van Houten H, Beenakker CWJ, Williamson JG, Kouwenhoven LP, van der Marel D, Foxon CT. 1988. Quantized conductance of point contacts in a two-dimensional electron gas. *Physical Review Letters* **60**: 848-850.

Vandersypen LMK, Elzerman JM, Schouten RN, Willems van Beveren LH, Hanson R, Kouwenhoven LP. 2004. Real-time detection of single-electron tunneling using a quantum point contact. *Applied Physics Letters* **85**: 4394-4396.

Wharam DA, Thornton TJ, Newbury R, Pepper M, Ahmed H, Frost JEF, Hasko DG, Peacock DC, Ritchie DA, Jones GAC. 1988. One-dimensional transport and the quantisation of the ballistic resistance. *Journal of Physics C: Solid State Physics* **21**: L209.